Multiple Run–Arrest Phenomena in Brittle Fracture

SUNDAR M. KAMATH
IBM General Technology Division, East Fishkill, New York 12533, USA

ABSTRACT

A special class of transient crack propagation problems arise from the interaction of stress waves with a rapidly moving crack. We study an extreme case in this class; namely, the repeated occurrence of sudden acceleration and intermittent crack arrests within a single test specimen. Using novel optical techniques, we have obtained real-time continuous measurements of the stress intensity factor and instantaneous crack-tip velocity during a series of run-arrest segments in brittle polymeric beams. Such observations provide new insights into the role of inertia effects in bending fracture.

KEYWORDS

Bending fracture; brittle fracture; crack arrest; crack propagation; optical method; stress wave.

INTRODUCTION

Contemporary studies in dynamic fracture have generally focused on steady-state crack growth as a means of extracting fundamental information on the mechanisms of the processes involved. This is mainly due to the analytic and experimental complexities inherent in any study of transient phenomena. For example, established techniques like high-speed photography are clearly incapable of capturing every detail of a highly transient process. Consequently, history effects, the influence of finite domains, and of non-uniform stress fields on dynamic crack propagation have not received adequate attention. In reality, however, non-uniform crack propagation is more likely in structural brittle fracture owing to the presence of stress wave reflectors like geometric discontinuities, and other sources of local stress variations such as welding residual stresses, changes in cross-section, and so on.

In this paper, we describe an effective experimental technique for

studying the dynamics of transient fracture, including extreme cases of sudden acceleration and intermittent arrest. Such a repeated sequence of rapid propagation followed by gradual arrest can be induced relatively easily and consistently in beam bending. The mechanics of brittle fracture in bending has been investigated by several researchers over the past 15 years or so (Bodner, 1973; Kinra and Kolsky, 1977; Dao and Herrmann, 1977; Schindler and Kolsky, 1983 among others). These studies, conducted mainly on glass and polymethylmethacrylate (PMMA) beams, served to highlight the important role played by reflected stress waves in bending fracture. They observed that, while the initial fracture propagated well beyond the original neutral axis of the beam, subsequent fracturing ensued only after the arrival of a longitudinal wave reflected from the far ends of the beam. Additional theoretical analyses (Freund and Herrman, 1976) reaffirmed the need for taking account of end reflections in bending fractures. Our study has revealed that another important factor is also involved, which turns out to be a surface or Rayleigh wave that emanates from the crack tip and travels back and forth along the traction-free crack face (Kamath and Kim, 1986).

Crack speed and wave propagation speed were the key parameters measured in all preceding experimental work, whereas the corresponding variation in stress intensity factor could not be obtained due to experimental limitations. This major shortcoming has been overcome in our work, so that it is now possible to record continuously and in real-time, the simultaneous variation of stress intensity factor and crack velocity during a highly transient fracture process. All transient measurements were performed in the total absence of high-speed photography.

EXPERIMENTAL DETAILS

Two transparent polymers were examined in this study, PMMA and Homalite-100, a polyester resin. Conventional fracture mechanics type notched bend bars were prepared from both polymers. The beams were of rectangular cross-section, approximately 6mm thick and 50mm deep, in two lengths, 230mm and 350mm. The extra long beam was chosen to delay wave reflection from the remote ends. Different initial notch root radii were incorporated in the test samples in order to vary the crack initiation conditions, and hence, the crack propagation speed and number of intermediate arrests. In addition to standard 1mm wide sawn notches, some extra wide 3mm notches were also prepared by milling; the purpose of the latter being to accommodate strain gages on the notch surface as a means of tracking the surface wave motion.

The notched beams were loaded in pure bending at room temperature in a screw-driven Instron machine at a nominal cross-head displacement rate of 0.5mm/min. Upon fracture initiation, the crack propagated in a brittle manner, so that total separation of the beam into two integral halves occurred within 200 to 1000 microseconds, depending upon initial conditions and beam length. The fracture propagated normal to the beam axis with no evidence of bifurcation at any stage.

During crack propagation, all variables central to the fracture process were continuously recorded in a digital transient recorder. The stress intensity factor and crack-tip velocity were measured using two newly developed optical techniques, while the motion of the three principal stress waves; namely, the longitudinal, flexural and surface waves, was monitored by strategically located resistance strain gages. Detailed

descriptions of the optical methods used to measure stress intensity factor (SIF) and crack-tip velocity may be found in Kamath, 1987.

Continuous Measurement of Dynamic SIF

The method used was the Stress Intensity Factor Tracer (SIFT) proposed originally by Kim, 1985. In the optical set-up, Fig. 1, a collimated beam of light is normally incident on the uncracked ligament in the test sample. On the other side, the transmitted light intensity is passed thru a special aperture and collected by a photomultiplier tube. The aperture is positioned at the focal plane of the second mirror. The SIF is related to the light intensity by the relation.

$$I = B\, K_I^{4/3}$$

where

$$B = 4/9\,\Omega_o D(cfd/(2\,\pi\,)^{1/2}\,)^{4/3}$$

and

$$D = \int_{\Gamma^*} (r'')^{-10/3}\, dS''$$

The geometrical shape factor D is calculated for the chosen aperture and Γ^* represents the total surface area where light collection occurs. The incident light intensity at the object plane Ω_o is designed to be constant, c is shadow-optic coefficient, f is focal length and d denotes sample thickness in the above relation. The output from the photo tube was recorded on a 12 bit 2 MHz Nicolet digital oscilloscope which was

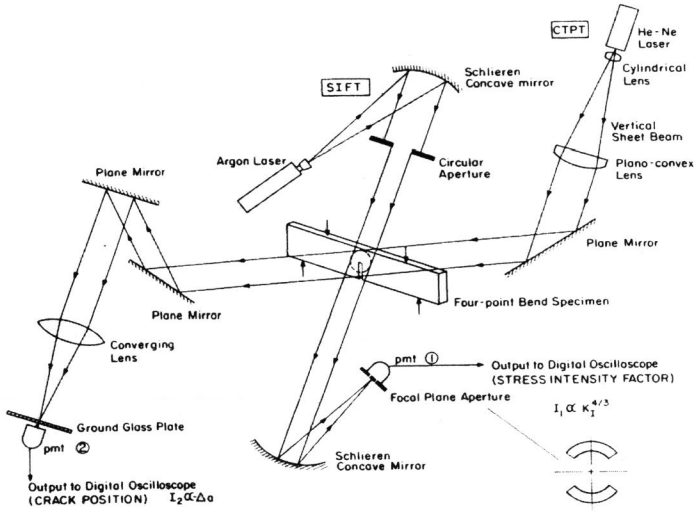

Fig. 1 Optical schemes for Stress Intensity Factor Tracer (SIFT) and crack-tip position detector used in continuous measurement of K and crack extension during transient brittle fracture in bending.

triggered a few microseconds prior to crack initiation. All digital data were transferred via a RS232C interface and processed on an IBM PC AT. A dynamic correction to the SIF computed from the above relation was applied as appropriate. Conversion of the SIFT signal (millivolts vs. microseconds) into SIF-time was achieved by a special calibration and numerical analysis scheme as described further in the dissertation referred to earlier (Kamath, 1987).

Continuous Measurement of Crack-Tip Velocity

Simultaneously with the SIFT signal, crack-tip position was recorded on another channel of the digital storage oscilloscope using the scheme indicated in Fig. 1. The basic idea is that a vertical sheet beam of light is made to obliquely intersect the center of the prospective fracture plane. As crack propagation occurs, the transmitted light intensity diminishes proportionately and a calibration of crack length can be made for the output intensity incident on the second photo tube. For linear variation, it is important to ensure constant and uniform intensity in the initial vertical sheet beam. The calibration and applicability of the technique was verified by using an independent measure of crack speed, i.e. by the conventional method based on a resistance grid of silver paint deposited on the sample surface to intersect the crack path.

Stress wave motion was tracked by standard strain gage techniques. For extensional and flexural waves, four-arm D.C. Wheatstone bridge circuits were used with the pair of active gages connected to opposite and adjacent arms respectively so that the modes are uncoupled. For the Rayleigh wave, or more specifically, the edge wave since the beam is of finite thickness, a single strain gage in a potentiometer circuit proved adequate.

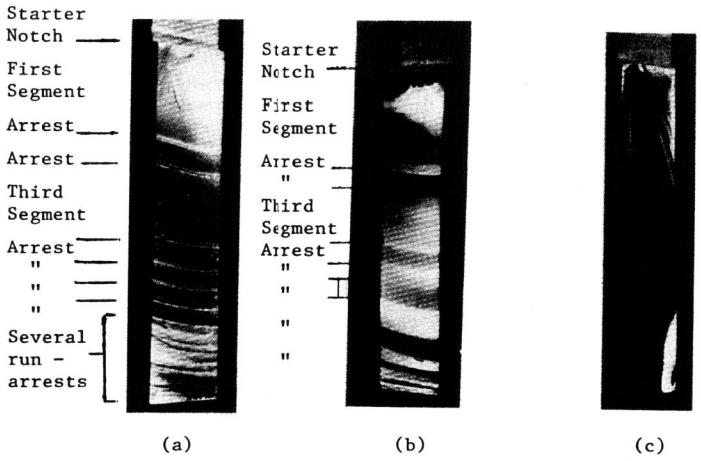

Fig. 2 Fracture surfaces of PMMA and Homalite beams showing multiple run-arrest segments (distinctly visible in PMMA). (a) PMMA test P4DL-26; (b) PMMA test P4DS-22; (c) Homalite test H3SS-34.

RESULTS AND DISCUSSION

A striking feature of the fracture pattern in bending, Fig. 2, is the presence of distinctly separated propagation segments. The actual number and size of such segments depend upon the material, the initiation SIF and the characteristic length scale governing wave reflections within the beam. While in PMMA the segments are clearly distinguishable, Figs. 2(a) and 2(b), this is not so in the case of Homalite 100, Fig. 2(c), except at high magnification when differences between the high and low velocity regions become discernible. Although several run-arrest units are obvious on the fracture surfaces shown for PMMA samples, our intention is to understand those first-order inertia effects which underlie the major segments. These turn out to be the first three segments, as marked in Figs. 2(a) and 2 (b); subsequent events become more difficult to analyze owing to the cumulative wave reflections from remote boundaries parallel and transverse to the crack plane, which leads to a complex series of closely-spaced run-arrest segments towards the end.

There were two main differences between tests P4DS-22 (or #22), and P4DL-26 (or #26). The nominal initiation SIF and beam length for P4DS-22 were 1.86 MPa$\sqrt{m}$ and 230mm, whereas for P4DL-26, the corresponding values were 1.57 MPa$\sqrt{m}$ and 350mm. Thus, with the exception of the notch root radius and the beam length, the two test samples were identical. The initiation SIF translates to a fracturing moment of 10.1 N-m for test #22 and 9.4 N-m for test #26. These differences led to some interesting variations in fracture behavior between the two tests. For example, the difference in initiation SIF resulted in dissimilar peak velocities and initial crack jumps; in test #22 the maximum crack velocity was close to 285 m/s and the first arrest occurred after 8.9mm of crack propagation. However, in test #26 the maximum velocity did not exceed 220 m/s and the initial arrest was at 7.4mm. It is important to note that, in spite of the distinct initial conditions, the time period for first arrest in both cases was close to, or slightly in excess of 50 microsecs. Another interesting piece of data is the time at which the third segment of rapid propagation commences. In the short beam sample (#22), this time period was roughly 120 microsecs after the first initiation. However, in the longer beam (#26), this interval was a little over 150 microsecs. The total time to fracture also varied in the two tests; thus, whereas 84% of the beam width was traversed in only 196 microsecs in test #22, a total of 1039 microsecs were needed for the crack to propagate thru 95% of the beam width in test #26.

All of the above features are clearly evident in the crack position versus time output obtained from the optical measurement scheme in Fig.1. An example of such output is reproduced here for test #22 in Fig. 3(b); careful differentiation of this digital output provides the velocity trace shown in Fig. 3(c). The corresponding variation in stress intensity factor as measured by the SIFT method during this highly transient fracture process is given in Fig. 3(a).

The afore-mentioned statistics relating to the time period of first arrest, and that for initiation of the third run segment can be meaningfully interpreted in the context of stress wave motion in the beam. A somewhat surprising and unique observation was the fact that the first arrest at approximately 50 microsecs following initiation, coincided with the arrival of a reflected Rayleigh-edge wave, based on a calculated plane stress wave speed of 1200 m/s for PMMA, and 1120 m/s for Homalite. This disturbance originates as an unloading pulse when the

crack first initiates and travels along the notch surfaces behind the crack-tip. Upon reaching the lateral surface of the beam it is reflected without change in phase, and returns to the moving crack-tip causing a

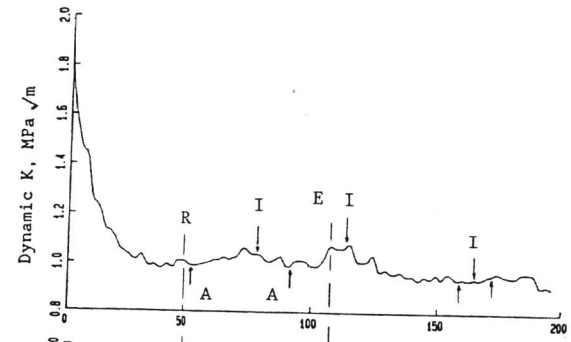

Fig. 3(a)

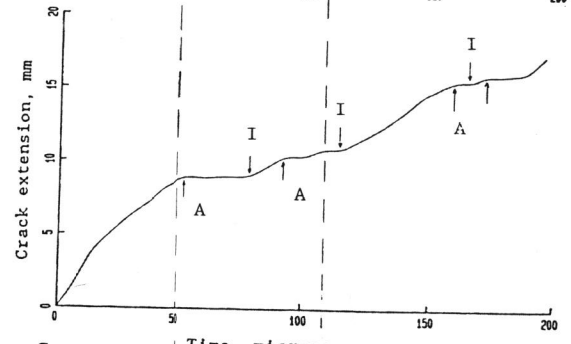

Fig. 3(b)

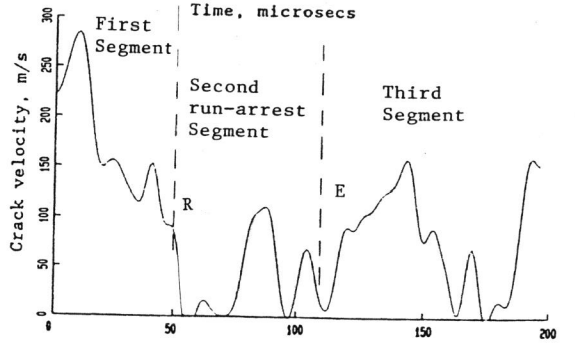

Fig. 3(c)

Fig. 3 Variation of (a) stress intensity factor, (b) crack-tip position, and (c) crack-tip velocity, during bending fracture in PMMA test P4DS-22. I- initiation; A - arrest; E - extensional wave arrival; R - Rayleigh wave arrival.

relatively sharp drop in the crack speed, as seen in Fig. 3(c), due to a 'crack closure' phenomenon. The strain gage results which demonstrate the validity of this line of reasoning were published and discussed in some detail previously (Kamath and Kim, 1986). It may be noted from Fig. 3(a) that the reduction in SIF which accompanies the Rayleigh wave-induced velocity decrease is comparatively small. This is to be expected since at these low velocities, the material toughness is a weak function of velocity, i.e., in the linear portion of the K-v curve small changes in SIF lead to non-proportionally large changes in velocity. Our observation is also consistent with preliminary deductions from a basic theoretical calculation (Freund, 1981).

As noted in the Introduction, previous studies have alluded to the strong influence of extensional waves in propagating the fracture well beyond the neutral axis of the beam. Our measurements confirm this to be the case, and in addition, we are able to observe the variation in SIF as well as velocity when the reflected wave interacts with the dormant crack front. When the fracture initiates for the first time, an unloading extensional wave propagates along the beam axis at essentially the bar wave velocity, which is 2140 m/s for PMMA and 1980 m/s for Homalite based on dynamic modulus. On reflection from the traction-free ends of the beam, the wave returns as a tensile front and causes the third run segment mentioned earlier. The arrival times are consistent with the different initiation times for the short and long beams. The increases in velocity and SIF indicated in Figs. 3(c) and (a) once again correspond with the expected variation in the stem of the material K-v curve. The actual extensional gage output for test #22 is shown in Fig. 4 and the period of oscillation is the same as the fundamental mode of free vibration for the half-beam.

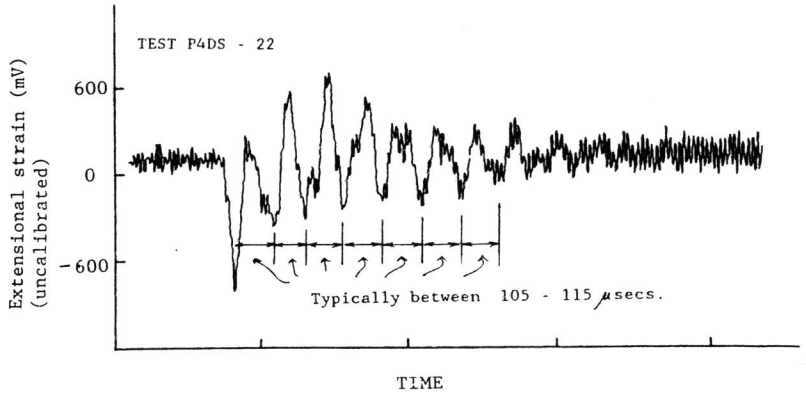

Fig. 4 Output of extensional wave strain gage during bending fracture in PMMA beam, test P4DS-22.

We have focused on the first and third run-arrest segments as being the major features of interest in this discussion. The short second segment is most likely associated with cylindrical wave reflection from the lateral front surface. However, this cannot be confirmed from the present work. In general, we found that the role of flexural waves was relatively insignificant compared to extensional waves, which is probably

due to the lower propagation speed and large attenuation associated with the flexural wave. While the results presented here all pertain to PMMA test samples, the same qualitative features extend to Homalite with respect to the velocity reduction induced by Rayleigh-edge waves, and the re-initiation caused by the reflected extensional wave. Details of the Homalite results are excluded owing to space limitations.

CONCLUDING REMARKS

This study has demonstrated that it is now possible to conduct detailed experimental studies of the mechanics of highly transient brittle fracture. Novel optical techniques like the Stress Intensity Factor Tracer can be used very effectively in this particularly difficult area of experimental mechanics. The specific case of bending fracture in a quasi-statically loaded finite beam was investigated. The results indicate the significant roles of the Rayleigh-edge wave and the extensional wave in the formation of multiple run-arrest segments in the brittle fracture of polymeric beams.

ACKNOWLEDGEMENTS

This work was completed when the author was a graduate student in Theoretical and Applied Mechanics at the University of Illinois at Urbana-Champaign. The advice and encouragement of Prof. Kyung-Suk Kim, thesis advisor, is gratefully acknowledged. Support was provided in the form of an IBM Pre-Doctoral Fellowship, and by the Research Board, UIUC, and the TAM Department.

REFERENCES

Bodner, S. R. (1973). Stress waves due to fracture of glass in bending. J. Mech. Phys. Solids, 21, 1-8.

Dao, K. and Herrmann, G., (1977). An experimental study of crack propagation in beams during fracture in bending. Proc. Int. Conf. Frac. Mech. Tech., Hong Kong ed. G. C. Sih, 1265-1279.

Freund, L. B. (1981). Influence of the reflected Rayleigh wave on a propagating edge crack. Int. J. Frac., 17, R83-86.

Freund, L. B. and Herrmann, G., (1976). Dynamic fracture of a beam or plate in plane bending. J. Appl. Mech., 43, 112-116.

Kamath, S. M. (1987). Some aspects of the mechanics and mechanisms of dynamic brittle fracture. Ph.D. Dissertation, Univ. of Illinois at Urbana-Champaign. Available from Univ. Microfilms, Ann Arbor, MI (Ref. #8721673).

Kamath, S. M. and Kim, K. S. (1986). On Rayleigh wave emissions in brittle fracture. Int. J. Frac., 31, R57-62.

Kim, K. S. (1985). A stress intensity factor tracer. J. Appl. Mech., 52, 291-297.

Kinra, V. K. and Kolsky, H. (1977). The interaction between bending fractures and the emitted stress waves. Eng. Frac. Mech., 9 423-432.

Schindler, H. J. and Kolsky, H. (1984). Instabilities in the fracture of brittle beams under flexural loading. Proc. Third Conf. Mech. Prop. High Rates of Strain. Inst. Phys. Conf. Ser. 70, Oxford, 299-306.